PROCEEDINGS OF SPIE

SPIEDigitalLibrary.org/conference-proceedings-of-spie

MAVIS: astrometric calibration technique

Jesse Cranney, Dionne Haynes, Israel Vaughn, Trevor Mendel, Stephanie Monty, et al.

Jesse Cranney, Dionne Haynes, Israel Vaughn, Trevor Mendel, Stephanie Monty, Davide Greggio, David Brodrick, François Rigaut, "MAVIS: astrometric calibration technique," Proc. SPIE 12185, Adaptive Optics Systems VIII, 1218567 (29 August 2022); doi: 10.1117/12.2629678

SPIE.

Event: SPIE Astronomical Telescopes + Instrumentation, 2022, Montréal, Québec, Canada

MAVIS: Astrometric calibration technique

Jesse Cranney[a,b], Dionne Haynes[a,b], Israel Vaughn[a,b], Trevor Mendel[a,b], Stephanie Monty[a,b], Davide Greggio[c], David Brodrick[a,b], and François Rigaut[a,b]

[a]Advanced Instrumentation and Technology Centre,
Research School of Astronomy and Astrophysics, the Australian National University,
Mount Stromlo Observatory, Weston ACT 2611, Australia
[b]Astralis Instrumentation Consortium, Australia
[c]INAF – Osservatorio Astronomico di Padova,
Vicolo dell'Osservatorio 5, 35122 Padova, Italy

ABSTRACT

The MCAO Assisted Visible Imager and Spectrograph (MAVIS) is currently in preliminary design for the ESO VLT in Chile, and is set to deliver diffraction limited science in V-band over a wide (30"x30") field of view. In order for MAVIS to capitalise on its high angular resolution over a large science field, a sensitive astrometric calibration process will be employed. The stringent requirements on this calibration process require the development of an astrometric calibration technique which is insensitive to manufacturing errors in the calibration mask, while still able to detect a broad range of distortions present in the MAVIS optical path. We derive one such calibration method along with simulations in the MAVIS context, using the open-source MAVISIM tool with realistic errors present.

Keywords: MAVIS, calibration, astrometry

1. INTRODUCTION

MAVIS[1] will provide wide-field (30×30 arcsec) images in V-band, sampled on a 4k×4k detector at 7.36 milliarcsec per pixel, fully utilising the ESO VLT's 8 metre aperture. In order to capitalise on this performance, MAVIS will deliver a post-calibration astrometric accuracy of:

- better than 150 microarcsec (goal of 50 microarcsec) for any objects separated by less than 1 arcsec (i.e., *relative astrometric accuracy*), and
- better than 2 milliarcsec (0.4 milliarcsec goal) for any object in the field (i.e., *absolute astrometric accuracy*).

In order to reach these astrometric requirements*, MAVIS will need to self-calibrate any residual distortions introduced by its own optical components, down to a tighter tolerance than those set by the requirements.

Astrometric calibration has been performed using on-sky data for a number of other instruments, including GEMS[2] and Hubble's WFPC2.[3] In these cases, distortions are classified using observations of star clusters. For GeMS, the prior knowledge of position of reference stars in the cluster is used to solve a least squares optimisation, ultimately delivering the distortion field as a set of coefficients of a set of basis functions. In the case of WFPC2, many dithered exposures of a cluster were taken, allowing the distortions to be reconstructed without precise prior knowledge of the reference star positions. These methods are both limited by the availability of appropriate star clusters on-sky, and the fact that the calibration process is not a controlled aspect of the instrument itself.

Another method of self-calibration is to include a removable *calibration mask* at a focal-plane before the entrance of an instrument, then measure the distortions as they appear from the science detector plane (e.g., using the science imager). By accurately knowing the positions of the calibration sources in the mask beforehand, it is

Send correspondence to Jesse Cranney, e-mail: jesse.cranney@anu.edu.au
*These requirements are only active when enough reference stars are available to calibrate plate scale and rotation.

Adaptive Optics Systems VIII, edited by Laura Schreiber, Dirk Schmidt, Elise Vernet,
Proc. of SPIE Vol. 12185, 1218567 · © 2022 SPIE
0277-786X · doi: 10.1117/12.2629678

possible to directly measure the field distortions introduced by the instrument. This is the method proposed for MICADO by Rodeghiero et al.[4] One drawback of this method is that the calibration mask must be manufactured to prohibitively difficult tolerances, as is concluded in Ref. 4.

In this paper, we discuss the details of a novel *differential* astrometric calibration procedur proposed for the MAVIS instrument, which utilises a calibration mask (as in MICADO), but allows relaxation of the tolerancing in the pinhole positions within the mask. In Section 2, we present the motivation and methodology behind our method. In Section 3, we give end-to-end simulation results verifying approach. In Section 4, we discuss the simulation results and propose future work to be done in the context of MAVIS astrometric calibration.

2. DIFFERENTIAL METHOD

2.1 Concept and Terminology

Firstly, a brief note on terminology; The distortion field we wish to identify is a vector valued function of x and y, $\mathbf{d} : \mathbb{R}^2 \to \mathbb{R}^2$. Without loss of generality, we can decompose the vector-valued distortion field, $\mathbf{d}$, into its x and y distortion components, i.e., $d_x : \mathbb{R}^2 \to \mathbb{R}$ and $d_y : \mathbb{R}^2 \to \mathbb{R}$, such that:

$$\mathbf{d}(\mathbf{p}) = \langle d^x(\mathbf{p}), d^y(\mathbf{p}) \rangle \tag{1}$$

Note that we use boldface Latin variables for vectors, capital Latin variables for matrices, and lowercase (unbolded) Latin variables for scalars. In this paper, we aim to recover the partial derivatives of each component of the distortion field with respect to x and y. The full set of partial derivatives we are interested in is:

$$\frac{\partial d_x}{\partial x}, \frac{\partial d_x}{\partial y}, \frac{\partial d_y}{\partial x}, \frac{\partial d_y}{\partial y}, \tag{2}$$

which when arranged into a matrix, form the Jacobian of the distortion:

$$\mathrm{J} \triangleq \begin{bmatrix} \frac{\partial d_x}{\partial x} & \frac{\partial d_x}{\partial y} \\ \frac{\partial d_y}{\partial x} & \frac{\partial d_y}{\partial y} \end{bmatrix} = \begin{bmatrix} \nabla^{\mathrm{T}} d_x \\ \nabla^{\mathrm{T}} d_y \end{bmatrix} \tag{3}$$

where ∇ is the gradient operator. Knowing the Jacobian of the distortion defines the distortion down to a set of constants. Those constants, in this case, are the global tip and tilt distortions, i.e., a constant offset in x and y across the field (which we do not aim to identify, as it does not impact the astrometric performance).

2.2 Measuring the Distortion Jacobian

The differential method of astrometric calibration aims to identify the Jacobian of the distortion field (or indeed, the gradient of the x and y components of the distortion field), rather than the distortion field itself.

In practice, this is performed by taking multiple exposures of a calibration mask, where the calibration mask is shifted slightly between each exposure. The measured difference in position compared to the expected difference in position gives an indication of the Jacobian of the distortion field near the pinhole position.

Formally, we can let the precise position of the pinholes in the calibration mask be:

$$\mathbf{p}_i = \langle x_i, y_i \rangle, \tag{4}$$

for $i \in [1, 2, ..., N_{\mathrm{pinholes}}]$. This is related to the nominal position of the pinholes, $\hat{\mathbf{p}}_i$, by:

$$\mathbf{p}_i = \hat{\mathbf{p}}_i + \mathbf{v}_i, \tag{5}$$

where $\mathbf{v}_i$ is the unknown error in pinhole position caused by, e.g., manufacturing errors, thermal fluctuations, *etc.*.

Now, the observed position, $\mathbf{q}_i$, of the pinhole through an optical system is defined as the true position, $\mathbf{p}_i$, perturbed by some distortion $\mathbf{d}_i$, as well as some measurement error, $\mathbf{w}_i$ (due to, e.g., centroiding error):

$$\mathbf{q}_i \triangleq \mathbf{p}_i + \mathbf{d}_i + \mathbf{w}_i. \tag{6}$$

Here, $\mathbf{d}_i$ is a sample of the continuous distortion field, $\mathbf{d} : \mathbb{R}^2 \to \mathbb{R}^2$, at the true pinhole position, i.e.,

$$\mathbf{d}_i = \mathbf{d}(\mathbf{p}_i) = \langle d_x(x_i, y_i), d_y(x_i, y_i) \rangle. \tag{7}$$

An *absolute* astrometric calibration process would aim to form an estimate, $\hat{\mathbf{d}}$, of the distortions from the measured positions, $\mathbf{q}_i$, compared to the assumed/ideal positions, denoted $\hat{\mathbf{p}}_i$:

$$\begin{aligned} \hat{\mathbf{d}}_i &= \mathbf{q}_i - \hat{\mathbf{p}}_i \\ &= \mathbf{q}_i - \mathbf{p}_i + \mathbf{v}_i \\ &= \mathbf{d}_i + \mathbf{v}_i + \mathbf{w}_i, \end{aligned} \tag{8}$$

which results in an error in distortion measurements exactly equal to the error in the pinhole positions, $\mathbf{v}_i$, plus the centroiding error, $\mathbf{w}_i$, exactly as one would expect.

For a *differential* method, we propose that one should make several observations of pinhole positions after shifting the calibration mask by a known amount. For simplicity, we will assume that exactly three shifts are applied and corresponding measurements are taken, though the method is generalisable to more measurements. The three sets of measurements are:

(i) $\mathbf{q}_i^0$, the reference measurement (with no shifts applied),

(ii) $\mathbf{q}_i^x$, a measurement after a shift in the x-direction, and

(iii) $\mathbf{q}_i^y$, a measurement after a shift in the y-direction.

That is,

$$\mathbf{q}_i^0 = \mathbf{p}_i + \mathbf{d}(\mathbf{p}_i) + \mathbf{w}_i^0 \tag{9}$$

$$\mathbf{q}_i^x = \mathbf{p}_i + \mathbf{s}_x + \mathbf{d}(\mathbf{p}_i + \mathbf{s}_x) + \mathbf{w}_i^x \tag{10}$$

$$\mathbf{q}_i^y = \mathbf{p}_i + \mathbf{s}_y + \mathbf{d}(\mathbf{p}_i + \mathbf{s}_y) + \mathbf{w}_i^y \tag{11}$$

where:

$$\mathbf{s}_x \triangleq \langle \Delta x, 0 \rangle \tag{12}$$

$$\mathbf{s}_y \triangleq \langle 0, \Delta y \rangle \tag{13}$$

In order to estimate the Jacobian of the distortion field, one can make the approximation:

$$\mathrm{J}_i \triangleq \mathrm{J}|_{\mathbf{p}=\mathbf{p}_i} \approx \hat{\mathrm{J}}_i \triangleq \begin{bmatrix} (\mathbf{q}_i^x - \mathbf{q}_i^0 - \mathbf{s}_x) \cdot \mathbf{e}_x / \Delta x & (\mathbf{q}_i^x - \mathbf{q}_i^0 - \mathbf{s}_x) \cdot \mathbf{e}_y / \Delta x \\ (\mathbf{q}_i^y - \mathbf{q}_i^0 - \mathbf{s}_y) \cdot \mathbf{e}_x / \Delta y & (\mathbf{q}_i^y - \mathbf{q}_i^0 - \mathbf{s}_y) \cdot \mathbf{e}_y / \Delta y \end{bmatrix} \tag{14}$$

where $\mathbf{e}_x$ and $\mathbf{e}_y$ are the basis vectors in the x and y dimensions, respectively. Examining only the first element of the estimated Jacobian for demonstrative purposes:

$$\left.\widehat{\frac{\partial d_x}{\partial x}}\right|_{\mathbf{p}=\hat{\mathbf{p}}_i} = \frac{(\mathbf{q}_i^x - \mathbf{q}_i^0 - \mathbf{s}_x) \cdot \mathbf{e}_x}{\Delta x} \tag{15}$$

$$= \frac{(\mathbf{d}(\mathbf{p}_i + \mathbf{s}_x) - \mathbf{d}(\mathbf{p}_i) + \mathbf{w}_i^x - \mathbf{w}_i^0) \cdot \mathbf{e}_x}{\Delta x}, \tag{16}$$

$$= \underbrace{\left(\frac{\mathbf{d}(\mathbf{p}_i + \mathbf{s}_x) - \mathbf{d}(\mathbf{p}_i)}{\Delta x} \right) \cdot \mathbf{e}_x}_{\to \left.\frac{\partial d_x}{\partial x}\right|_{\mathbf{p}=\mathbf{p}_i}, \text{ as } \Delta x \to 0} + \left(\frac{\mathbf{w}_i^x - \mathbf{w}_i^0}{\Delta x} \right) \cdot \mathbf{e}_x, \tag{17}$$

one can see that as $\Delta x \to 0$, the first term in Eqn. (17) tends to be the exact entry of the true Jacobian, while simultaneously, the second term tends to infinity. This reveals that there is a clear trade-off between accuracy of the Jacobian in this formalism, and the measurement error of the pinhole positions (e.g., centroiding error). Note however that the pinhole position error, $\mathbf{v}_i$, does not enter this relationship. The only impact of $\mathbf{v}_i$ on the Jacobian estimation is that the Jacobian is in fact being sampled at a slightly displaced position than the nominal position; The Jacobian estimate is at $\mathbf{p}_i = \hat{\mathbf{p}}_i + \mathbf{v}_i$, but we assume that that it is at the ideal pinhole positions, $\hat{\mathbf{p}}_i$. Assuming that $\mathbf{d}(\mathbf{p}_i) \approx \mathbf{d}(\hat{\mathbf{p}}_i)$, then this will not have any significant impact on the distortion recovery.

2.3 Estimating the Distortion

After the Jacobian has been sampled across the field, the remaining task is to determine a set of distortions that are compatible with the measured Jacobian samples. For this, we require a set of differentiable basis functions, $f_n(\mathbf{p}), g_n(\mathbf{p}),\ n \in [1, 2, \ldots, N]$, and assume that the distortion field is the linear combination of these basis functions:

$$d_x(\mathbf{p}) = \sum_{n=1}^{N} a_n f_n(\mathbf{p}), \tag{18}$$

$$d_y(\mathbf{p}) = \sum_{n=1}^{N} b_n g_n(\mathbf{p}). \tag{19}$$

The Jacobian at a point $\mathbf{p}_i$ is then:

$$\mathrm{J}_i = \begin{bmatrix} \sum_{n=1}^{N} a_n \frac{\partial f_n}{\partial x}(\mathbf{p}_i) & \sum_{n=1}^{N} a_n \frac{\partial f_n}{\partial y}(\mathbf{p}_i) \\ \sum_{n=1}^{N} b_n \frac{\partial g_n}{\partial x}(\mathbf{p}_i) & \sum_{n=1}^{N} b_n \frac{\partial g_n}{\partial y}(\mathbf{p}_i) \end{bmatrix}, \tag{20}$$

which can be flattened into a column vector, in order to form the ensuing least-squares regression problem:

$$\mathbf{z}_i \triangleq \mathrm{vec}(\mathrm{J}_i), \tag{21}$$

$$= \begin{bmatrix} \sum_{n=1}^{N} a_n \frac{\partial f_n}{\partial x}(\mathbf{p}_i) \\ \sum_{n=1}^{N} b_n \frac{\partial g_n}{\partial x}(\mathbf{p}_i) \\ \sum_{n=1}^{N} a_n \frac{\partial f_n}{\partial y}(\mathbf{p}_i) \\ \sum_{n=1}^{N} b_n \frac{\partial g_n}{\partial y}(\mathbf{p}_i) \end{bmatrix}, \tag{22}$$

$$= \underbrace{\left[\begin{array}{cccc:cccc} \frac{\partial f_1}{\partial x}(\mathbf{p}_i) & \frac{\partial f_2}{\partial x}(\mathbf{p}_i) & \cdots & \frac{\partial f_N}{\partial x}(\mathbf{p}_i) & 0 & 0 & \cdots & 0 \\ 0 & 0 & \cdots & 0 & \frac{\partial g_1}{\partial x}(\mathbf{p}_i) & \frac{\partial g_2}{\partial x}(\mathbf{p}_i) & \cdots & \frac{\partial g_N}{\partial x}(\mathbf{p}_i) \\ \hdashline \frac{\partial f_1}{\partial y}(\mathbf{p}_i) & \frac{\partial f_2}{\partial y}(\mathbf{p}_i) & \cdots & \frac{\partial f_N}{\partial y}(\mathbf{p}_i) & 0 & 0 & \cdots & 0 \\ 0 & 0 & \cdots & 0 & \frac{\partial g_1}{\partial y}(\mathbf{p}_i) & \frac{\partial g_2}{\partial y}(\mathbf{p}_i) & \cdots & \frac{\partial g_N}{\partial y}(\mathbf{p}_i) \end{array}\right]}_{D_i} \underbrace{\left[\begin{array}{c} a_1 \\ a_2 \\ \vdots \\ a_N \\ \hdashline b_1 \\ b_2 \\ \vdots \\ b_N \end{array}\right]}_{\mathbf{u}}. \tag{23}$$

Then, in a similar fashion, one can define the vectorised estimated Jacobian at the same point as:

$$\hat{\mathbf{z}}_i = \mathrm{vec}(\hat{J}_i) \tag{24}$$

$$= \begin{bmatrix} (\mathbf{q}_i^x - \mathbf{q}_i^0 - \mathbf{s}_x) \cdot \mathbf{e}_x / \Delta x \\ (\mathbf{q}_i^y - \mathbf{q}_i^0 - \mathbf{s}_y) \cdot \mathbf{e}_x / \Delta y \\ (\mathbf{q}_i^x - \mathbf{q}_i^0 - \mathbf{s}_x) \cdot \mathbf{e}_y / \Delta x \\ (\mathbf{q}_i^y - \mathbf{q}_i^0 - \mathbf{s}_y) \cdot \mathbf{e}_y / \Delta y \end{bmatrix}. \tag{25}$$

Now we can formulate an optimisation problem to fit the observed Jacobian samples to the true Jacobian samples as a function of the linear combination coefficients:

$$\text{cost} \triangleq \sum_{i=1}^{N_{\text{pinholes}}} \|\hat{\mathbf{z}}_i - \mathbf{z}_i\|^2, \tag{26}$$

$$= \sum_{i=1}^{N_{\text{pinholes}}} \|\hat{\mathbf{z}}_i - D_i\mathbf{u}\|^2, \tag{27}$$

$$= \left\| \underbrace{\begin{bmatrix} \hat{\mathbf{z}}_1 \\ \hat{\mathbf{z}}_2 \\ \vdots \\ \hat{\mathbf{z}}_{N_{\text{pinholes}}} \end{bmatrix}}_{\hat{\mathbf{z}}} - \underbrace{\begin{bmatrix} D_1 \\ D_2 \\ \vdots \\ D_{N_{\text{pinholes}}} \end{bmatrix}}_{D} \mathbf{u} \right\|^2, \tag{28}$$

$$= \|\hat{\mathbf{z}} - D\mathbf{u}\|^2, \tag{29}$$

where $\|\cdot\|$ is the Euclidean-norm operator. This cost function is minimised by:

$$\hat{\mathbf{u}} = \text{argmin}_{\mathbf{u}}\,(\text{cost}) = \left(D^{\mathrm{T}}D\right)^{-1} D^{\mathrm{T}}\hat{\mathbf{z}}, \tag{30}$$

assuming $D^{\mathrm{T}}D$ is positive definite (which can be guaranteed by choice of pinhole positions and basis functions).

So, given the Jacobian measurements, $\hat{\mathbf{z}}$, it is possible to estimate the distortion field basis function coefficients, $\hat{\mathbf{z}}$. Note that the inversion in Eqn. (30) only needs to be computed once per system geometry (pinhole positions and choice of basis functions), and then can be reused for all future observations.

2.4 Distortion Basis Functions

As mentioned in Section 2.3, the distortion field is assumed to be a linear combination of differentiable basis functions. For this paper, we use a set of bi-variate homogeneous polynomials for the distortion basis functions, of the form:

$$p_{n,m}(x, y) = \frac{1}{n!} x^{n-m} y^m \tag{31}$$

where $m \in [0, 1, \cdots, n]$, $n \in [0, 1, \cdots, N_{\text{order}}]$, and N_{order} determines the largest exponent seen in the basis functions. The factor of $1/n!$ is included to improve the conditioning of $D^{\mathrm{T}}D$ in Eqn. (30). For this choice of basis, there are:

$$N = \frac{(N_{\text{order}} + 1)(N_{\text{order}} + 2)}{2} - 1$$

unique polynomial functions. This includes the removal of the constant term, so that the minimum polynomial order is 1. It can be shown that using the method described above, there is no information about the constant value, and as such, it cannot be included in the estimation process. In fact, since all derivatives of this function are precisely equal to 0, the corresponding columns of D would also be zero, guaranteeing that $D^{\mathrm{T}}D$ is not positive-definite.

It is not clear if this choice of polynomial functions is optimal. In fact, the Legendre polynomials have been observed to be more stable in distortion identification.[2,5] Alternative basis functions will be explored in the development of the MAVIS calibration unit.

3. SIMULATIONS

In order to validate the proposed astrometric calibration process, simulations were developed, based on (and now included in) the MAVIS image simulator, MAVISIM.[6] These simulations were designed with speed in mind, in order to rapidly evaluate different system parameters, noise characteristics, and distortion inputs. As such, they assume that the pinhole positions and centroiding error follow Gaussian statistics, that is:

$$\mathbf{v}_i \sim \mathcal{N}\left(\begin{bmatrix} 0 \\ 0 \end{bmatrix}, \begin{bmatrix} \sigma_v^2 & 0 \\ 0 & \sigma_v^2 \end{bmatrix}\right), \tag{32}$$

$$\mathbf{w}_i \sim \mathcal{N}\left(\begin{bmatrix} 0 \\ 0 \end{bmatrix}, \begin{bmatrix} \sigma_w^2 & 0 \\ 0 & \sigma_w^2 \end{bmatrix}\right). \tag{33}$$

The distortion fields were generated using statistical methods based on the MAVIS design, as presented in a companion paper by Greggio et al.[7] Then, the process described in Section 2 is executed for particular choices of:

- Calibration mask shift $(\Delta x, \Delta y)$ of 0.2 arcsec ($\sim$0.12 mm),
- Polynomial maximum order (N_{order}) of 6.
- Pinhole position error ($\mathbf{v}_i$) of 0.2 arcsec ($\sim$0.12 mm),
- Centroid measurement error ($\mathbf{w}_i$) of 10 microarcsec ($\sim$5.8 microns),

The first two terms (shift size and polynomial order) were found to give stable results, but are not precisely optimised. The last two terms (pinhole position and centroid accuracy) are based on conservative estimates given the MAVIS design.

By choosing appropriate values of these parameters, we were able to verify the ability of the differential astrometric calibration method to identify distortions to a very high precision (when average field tip-tilt is removed, since they are not in the astrometric error budget). We show that for a typical MAVIS distortion field, we are able to reduce the field distortions to below the required astrometric requirement levels. Figure 1 shows the simulated field distortions before and after calibration using the differential astrometric calibration method.

This gives a good indication of the performance of the method proposed in this paper, but it does not directly inform the astrometric requirements of MAVIS. For that, we simulate a large number of random objects in the MAVIS field-of-view, and determine the astrometric error of these objects when subject to the post-calibration residual distortions. Figure 2 shows the results.

For the relative astrometric accuracy, we appear to always satisfy the requirements (150 microarcsec for objects $\leq$1 arcsec apart), but not always the goal (50 microarcsec for objects $\leq$1 arcsec apart). For the absolute astrometric accuracy, we appear to always satisfy the requirements (2 milliarcsec anywhere in the field), and almost always satisfy the goal (0.4 milliarcsec anywhere in the field).

In the companion paper, Ref. 7, distortion calibration was investigated using the method described in this paper, and with some finer tuning than presented here, the MAVIS distortion field was able to be reduced to 66 microarcsec RMS over the MAVIS field of view (30 arcsec diameter disc). In that paper, the impact of using different polynomial orders was investigated, and it was concluded that for the homogeneous bi-variate polynomials described in Section 2.4 of this paper, $N_{\text{order}} = 11$ polynomials produced the best distortion fit.

Additionally, to verify the entire pipeline, an end-to-end simulator was developed (not included in MAVISIM). This tool generates images on a simulated CCD with realistic detector noise, then performs the entire pipeline of windowing, centroiding, and distortion fitting. As suspected, this simulation produced results very similar to those found in the simulation described above, albeit at a much longer execution time. An example calibration mask image generated in this simulation is shown in Fig. 3.

One critical aspect which is currently missing from these simulations is uncertainty in the shifting amount, $\Delta x, \Delta y$. We have performed initial investigations on this aspect, but will present the results in future work. Our

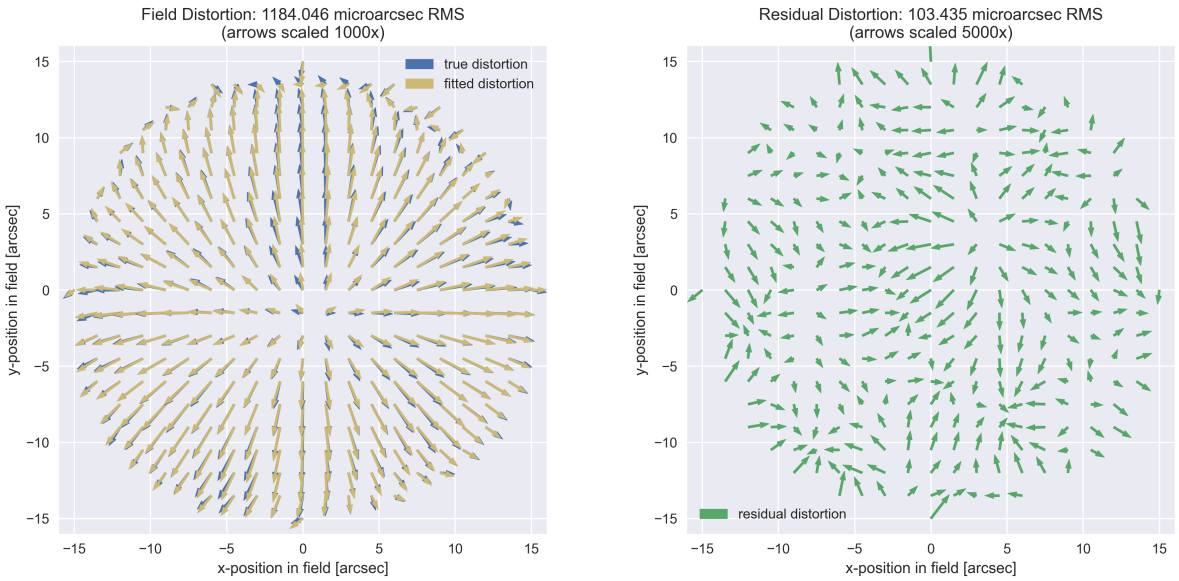

Figure 1. Simulated field distortions of MAVIS (red arrows), fitted distortions of MAVIS using the differential astrometric calibration method (blue arrows), residual distortion of MAVIS after calibration (green arrows). Note that the arrow scaling is different between the two plots.

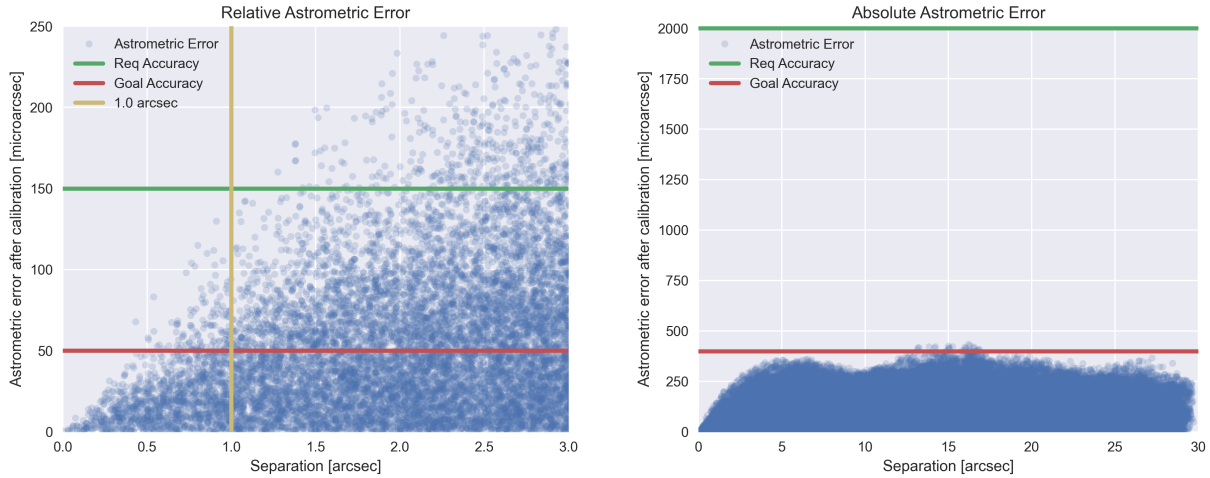

Figure 2. Expected post-calibration MAVIS astrometric performance with respect to MAVIS requirements. For the relative astrometric performance (left), no points should lie above the horizontal lines (to the left of the vertical line). For the absolute astrometric performance (right), no points should lie above the horizontal lines at any separation.

preliminary conclusions are that knowledge of the shifts is crucial for recovering plate-scale distortion modes, but when plate-scale distortion identification is not required (e.g., the MAVIS astrometric requirements, which specify the presence of on-sky reference stars to calibrate plate-scale) the knowledge of the shifts is not required. This is because the average shift of the measured pinhole positions can be assumed to be the shifting amount which allows for very accurate knowledge of the shifting amount, at the cost of removing any impact of plate-scale on the measured positions (since plate-scale has the effect of scaling the measured coordinates as a linear function of the field coordinates).

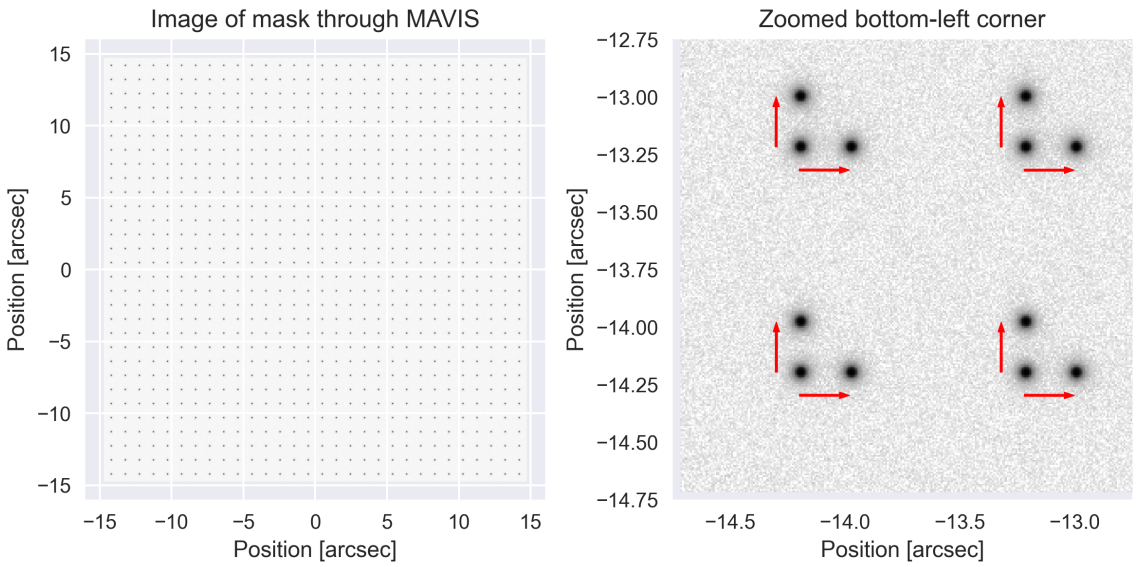

Figure 3. Simulated calibration mask (left), and zoom in on corner of calibration mask, with images after x and y shifts (red arrows) stacked for demonstration purposes (right).

4. CONCLUSIONS

Self-calibration is an increasingly popular feature of astronomical instruments which promise to deliver high astrometric performance. Manufacturing constraints result in the required astrometric calibration masks to be challenging to make. The differential astrometric calibration technique proposed in this paper allows for a high-precision distortion field to be recovered, with very little sensitivity to the manufacturing tolerance of the calibration mask. The use of this method in the context of MAVIS is expected to allow MAVIS to reach its required astrometric performance. With further tuning of calibration system parameters and choice of distortion basis functions, it may even be possible to exceed the astrometric performance goals. Additional simulations are also required to assess the impact of shifting errors on plate-scale distortion identification.

REFERENCES

[1] Rigaut, F. et al., "MAVIS conceptual design," in [*Ground-based and Airborne Instrumentation for Astronomy VIII*], Evans, C. J., Bryant, J. J., and Motohara, K., eds., **11447**, SPIE (2020).

[2] Bernard, A., Neichel, B., Mugnier, L. M., and Fusco, T., "Optimal correction of distortion for high-angular-resolution images: Application to GeMS data," *MNRAS* **473** (nov 2017).

[3] Anderson, J. and King, I., "An Improved Distortion Solution for the Hubble Space Telescope's WFPC2," *Publications of the Astronomical Society of the Pacific* **115** (2003).

[4] Rodeghiero, G., Sawczuck, M., Pott, J.-U., Glück, M., Biancalani, E., Häberle, M., Riechert, H., Pernechele, C., Naranjo, V., Moreno-Ventas, J., Bizenberger, P., Perera, S., and Lessio, L., "Development of the warm astrometric mask for MICADO astrometry calibration," *Publications of the Astronomical Society of the Pacific* **131** (2019).

[5] Service, M., Lu, J. R., Campbell, R., Sitarski, B. N., Ghez, A. M., and Anderson, J., "A new distortion solution for NIRC2 on the keck II telescope," *Publications of the Astronomical Society of the Pacific* **128** (2016).

[6] Monty, S., Rigaut, F., McDermid, R., Baumgardt, H., Cranney, J., Agapito, G., Mendel, J. T., Plantet, C., Greggio, D., Stetson, P. B., Fiorentino, G., and Haynes, D., "Towards realistic modelling of the astrometric capabilities of MCAO systems: detecting an intermediate-mass black hole with MAVIS," *MNRAS* **507** (2021).

[7] Greggio, D. et al., "MAVIS Adaptive Optics Module: optical configuration and expected performance," in [*Astronomical Telescopes and Instrumentation*], *Proc. SPIE* (2022).